Green's function approach to quantum criticality in the anisotropic Kondo necklace model

H. Rezania and A. Langari*
Physics Department, Sharif University of Technology, Tehran 11155-9161, Iran

P. Thalmeier
Max Planck Institute for Chemical Physics of Solids, 01187 Dresden, Germany

(Received 19 December 2007; published 28 March 2008)

We have studied the quantum phase transition between the antiferromagnetic and spin liquid phases for the two-dimensional anisotropic Kondo necklace model. The bond operator formalism has been implemented to transform the spin Hamiltonian to a bosonic one. We have used the Green's function approach including a hard core repulsion to find the low energy excitation spectrum of the model. The bosonic excitations become gapless at the quantum critical point where the phase transition from the Kondo singlet state to long range antiferromagnetic order takes place. We have studied the effect of both intersite (δ) and local (Δ) anisotropies on the critical point and on the critical exponent of the excitation gap in the paramagnetic phase. We have also compared our results with previous bond operator mean field calculations.

DOI: 10.1103/PhysRevB.77.094438 PACS number(s): 75.10.Jm, 75.30.Mb, 75.30.Kz, 75.40.Mg

I. INTRODUCTION

The description of quantum phase transition between phases with spontaneously broken symmetry and disordered phases is a novel topic in condensed matter physics.[1,2] Macroscopic strongly correlated electron systems at low temperature (and as a function of magnetic field and hydrostatic or chemical pressure) show a wide range of interesting phenomena, such as quantum criticality and associated non-Fermi liquid (NFL) behavior, magnetism, Kondo insulating behavior, and superconductivity.[3,4] In the single-impurity case, the Kondo problem describes the antiferromagnetic interaction ($J_\perp$) between the impurity spin and the free conduction electron spins. This gives rise to a new nonperturbative low energy scale, the Kondo temperature T_K, which dominates the low temperature anomalies in the thermodynamic and transport quantities.[3] $T_K=De^{-1/(2J_\perp\rho)}$ (D and ρ are conduction band width and density of states, respectively) has the meaning of a crossover temperature from uncoupled local spins for $T\gg T_K$ to the strongly coupled local spins, forming a singlet ground state with conduction electrons, for $T\ll T_K$. In the Kondo lattice (KL) model,[5] an additional (perturbative) energy scale $T_{RKKY}=J_\perp^2\rho$ for the effective Ruderman–Kittel–Kasuya–Yosida (RKKY) intersite interactions of local spins appears. This model exhibits a quantum phase transition between the Kondo singlet phase and the magnetically ordered phase as function of the control parameter $x=J_\perp\rho(E_F)$, as argued by Doniach.[6] The transition takes place at a quantum critical point (QCP) characterized by $x_c=J_{\perp c}\rho(E_F)$, where x_c is of the order 1. For $x\ll x_c$, the effective interactions dominate and magnetic order appears. For $x\gg x_c$, the singlet formation dominates and a heavy Fermi liquid state is realized. This qualitative picture has been supported by numerical calculations within dynamical mean field theory and exact diagonalization methods[7,8] for the Anderson lattice and Kondo lattice Hamiltonians, respectively. However, the vicinity of the quantum critical point and associated NFL behavior[9] requires a treatment within phenomenological effective models, as developed in Refs. 10 and 11.

The Kondo lattice model emerges from the periodic Anderson model via a Schrieffer–Wolff transformation that eliminates the fluctuations of f-charge or f-orbital occupation.[5] It is given by

$$H_{KL}=t\sum_{\langle ij\rangle,\tau}(c_{i,\tau}^{\dagger}c_{j,\tau}+\text{H.c.})+J_\perp\sum_i\tau_i\mathbf{S}_i. \tag{1}$$

The first part describes conduction electrons $c_{i,\tau}^{\dagger}$ with nearest neighbor hopping t. The second part is the Kondo term where τ_i and $\mathbf{S}_i$ are conduction electron and localized spin, respectively. This model still contains the charge fluctuations of conduction electrons expressed by the hopping term. It was shown by Doniach[6] that in one dimension, it may be replaced by an xy-type intersite exchange term. Thus, the Kondo lattice model is replaced by a pure spin Hamiltonian, the Kondo necklace model (KNM). In higher dimension, this procedure cannot be justified strictly. However, suppose that we add a Coulomb repulsion U_c between conduction electrons to the KL model [Eq. (1)] in the half filled case. Then, in the limit $U_c/t\to\infty$, charge fluctuations of conduction electrons are frozen out and the low energy physics is again described by a pure spin Hamiltonian. Strictly speaking, this is only adequate for the Kondo insulator with a charge gap but one may expect that it is also useful to describe the low energy spin dynamics of metallic Kondo systems. The generalized Kondo necklace model obtained in this way[12] is given by

$$H=J\sum_{\langle i,j\rangle}(\tau_i^x\tau_j^x+\tau_i^y\tau_j^y+\delta\tau_i^z\tau_j^z)+J_\perp\sum_{\langle i\rangle}(\tau_i^xS_i^x+\tau_i^yS_i^y+\Delta\tau_i^zS_i^z), \tag{2}$$

where the intersite exchange J is of order t^2/U_c. In two dimensions, which will be considered in the present work, this is equivalent to a special case of a (anisotropic) bilayer-Heisenberg model[13] where the intersite bonds (J) are cut in one layer and $J_\perp$ is the interlayer coupling. Here, both spins are $1/2$ and the exchange coupling parameters are antiferromagnetic ($J,J_\perp\geqslant 0$). In the above Hamiltonian, τ_i^α represent

the α component of spin of the "itinerant" electrons at site i and S_i^α is the α component of localized spins at position i.

We want to study the possible quantum phase transition of this model under a rather general assumption of both anisotropies in the intersite interaction ($\sim J$) and on-site Kondo terms ($\sim J_\perp$) of Eq. (2). They are characterized by a pair of parameters (δ,Δ). The Δ anisotropy is always present in real Kondo compounds such as Ce-based intermetallics due to the crystalline electric field and δ is caused by spin-orbit coupling of conduction electrons. We study the quantum phase transition from the paramagnetic (Kondo singlet) side as a function of the control parameter $J_\perp/J$, which gives the ratio of the intersite to the on-site interaction strength, and as a function of the anisotropy parameters (δ,Δ). We have implemented the Green's function approach introduced to study the bilayer isotropic Heisenberg model $(\delta,\Delta)=(1,1)$.[13] The effect of anisotropies on the quantum phase transition of KNM has recently been studied by a mean field approach both in the absence[14] and presence[15] of a magnetic field. However, using the more advanced Green's function method, we will obtain more accurate values for the critical gap exponents ν and for quantum critical point values $(J_\perp/J)_c$ which differ both from the mean field values.

II. BOSON OPERATOR REPRESENTATION OF THE MODEL HAMILTONIAN

The bond operator representation introduced by Chubukov[16] and Sachdev and Bhatt[17] is a useful approach to describe disordered phases. This representation can be considered as an analog of the usual Holstein–Primakov transformation for phases with broken spin rotational symmetry. In terms of singlet-triplet operators, the spin operators of the localized and conduction electrons are given by

$$S_{i,\alpha}=\frac{1}{2}(s_i^\dagger t_{i,\alpha}+t_{i,\alpha}^\dagger s_i-i\epsilon_{\alpha\beta\gamma}t_{i,\beta}^\dagger t_{i,\gamma}),$$

$$\tau_{i,\alpha}=\frac{1}{2}(-s_i^\dagger t_{i,\alpha}-t_{i,\alpha}^\dagger s_i-i\epsilon_{\alpha\beta\gamma}t_{i,\beta}^\dagger t_{i,\gamma}), \tag{3}$$

where (α,β,γ) represent the (x,y,z) components and ϵ is the totally antisymmetric tensor. The bond operators satisfy bosonic commutation relations $[s_i,s_i^\dagger]=1$, $[t_{i,\alpha},t_{i,\beta}^\dagger]=\delta_{\alpha,\beta}$ and $[s_i,t_{i,\alpha}^\dagger]=1$. We will calculate the one particle boson Green's function using Feynman diagrams for triplet operators and find the excitation spectrum. Our calculations are for zero temperature. In order to ensure that the physical states are either singlets or triplets, one has to impose the constraint $s^\dagger s+\Sigma_\alpha t_\alpha^\dagger t_\alpha=1$ on every bond, where s (singlet) and t_α (triplet) are bond operators.

In Refs. 14 and 15, this has been implemented on a mean field level by introducing a chemical potential as Lagrange parameter. In this approach, average amplitudes $\bar{s}=\langle s_i\rangle$ and $\bar{t}=\langle t_{i\alpha}\rangle$ are introduced and their self-consistent solutions are found by minimizing the total ground state energy. Here, $\bar{t}\neq 0$ denotes a triplet condensed state with magnetic order. The chemical potential adjusts itself such that the average constraint $\bar{s}^2=1-\bar{t}^2$ is approximately satisfied. In fact, in the paramagnetic region ($\bar{t}=0$), it was found[14] that $\bar{s}$ is only a few percent below singlet saturation $\bar{s}=1$ even close to the QCP where triplet excitations become soft. The zero point energy of the latter contribute to the ground state energy. Since in the mean field approach the number of triplet bosons on a given bond is not constrained, there are contributions from unphysical states in the ground state energy.

In the present work, we are therefore using a more advanced implementation of the local constraint which can be written as $s_i^\dagger s_i=(1-\Sigma_\alpha t_{i\alpha}^\dagger t_{i\alpha})$. It may be satisfied if either $s_i^\dagger s_i=1$ and $\Sigma_\alpha t_{i\alpha}^\dagger t_{i\alpha}=0$ or $s_i^\dagger s_i=0$ and $\Sigma_\alpha t_{i\alpha}^\dagger t_{i\alpha}=1$. To project out unphysical states on every bond with more than one excited triplet, one has to require $\Sigma_\alpha t_{i\alpha}^\dagger t_{i\alpha}^\dagger=0$. This may be achieved by introducing an on-site repulsion U of triplet bosons,[13] which is then taken in the hard core limit $U\to\infty$, see Eq. (12) below. As starting point for noninteracting triplets, we use the unconstrained case with $s\to\bar{s}=1$ in Eq. (3). In the paramagnetic case which we consider here, this is well justified by the mean field result mentioned above. In principle, one might think of a combined approach keeping $\bar{s}$ as a variational parameter within the hard core boson approximation. We will discuss this further in Sec. VIII. This hard core boson approach can be applied to any model, for which the excitations in the disordered phase are triplets above a strong coupling singlet ground state. The Hamiltonian in Eq. (2) has three control parameters, $J_\perp$, δ, and Δ. Using the bond operator transformations in the Kondo necklace model of Eq. (2), we obtain the effective Hamiltonian

$$H=H_2+H_3+H_4, \tag{4}$$

where H_2 is the one particle part of the Hamiltonian. It is composed of two terms,

$$H_2=H_{J_\perp}+H_1, \tag{5}$$

where the exchange term $H_{J_\perp}$ is diagonal in terms of the bond operators and H_1 has pairing terms between boson triplets which results in nonconservation of the triplet bosons and the possible formation of a Bose–Einstein condensate of triplet bosons describing the magnetically ordered state. This term leads to a nonzero anomalous expectation value $\langle t_\alpha t_\alpha\rangle$ or corresponding anomalous Green's function. In terms of bond operators, $H_{J_\perp}$ and H_1 are given by

$$H_{J_\perp}=J_\perp\sum_i\left[\frac{(1+\Delta)}{2}[t_{i,x}^\dagger t_{i,x}+t_{i,y}^\dagger t_{i,y}]+t_{i,z}^\dagger t_{i,z}\right],$$

$$H_1=\frac{J}{4}\sum_{\langle i,j\rangle}\sum_{\alpha=x,y}[t_{i,\alpha}(t_{j,\alpha}+t_{j,\alpha}^\dagger)+\text{H.c.}]$$
$$+\frac{J\delta}{4}\sum_{\langle i,j\rangle}[t_{i,z}(t_{j,z}+t_{j,z}^\dagger)+\text{H.c.}]. \tag{6}$$

The other parts of the Hamiltonian which describe triplet boson interactions are represented by

$$H_3 = \frac{J}{4}\sum_{\langle i,j\rangle}\{i[(t_{i,x}+t_{i,x}^\dagger)(t_{j,y}^\dagger t_{j,z}-t_{j,z}^\dagger t_{j,y})+(t_{i,y}+t_{i,y}^\dagger)\times(t_{j,z}^\dagger t_{j,x}-t_{j,x}^\dagger t_{j,z})+\delta(t_{i,z}+t_{i,z}^\dagger)(t_{j,x}^\dagger t_{j,y}-t_{j,y}^\dagger t_{j,x})]+\text{H.c.}\}, \quad (7)$$

$$H_4 = -\frac{J}{4}\sum_{\langle i,j\rangle}[(t_{i,y}^\dagger t_{i,z}-\text{H.c.})(t_{j,y}^\dagger t_{j,z}-\text{H.c.})+(t_{i,x}^\dagger t_{i,z}-\text{H.c.})\times(t_{j,x}^\dagger t_{j,y}-\text{H.c.})+\delta(t_{i,x}^\dagger t_{i,y}-\text{H.c.})(t_{j,x}^\dagger t_{j,y}-\text{H.c.})]. \quad (8)$$

The Hamiltonian can be written in terms of triplet Fourier components, $t_{i,\alpha}=\frac{1}{\sqrt{N}}\Sigma_{\mathbf{k},\alpha}t_{k,\alpha}e^{i\vec{k}\cdot\vec{R}_i}$, leading to the quadratic form

$$H_2 = \sum_{k,\alpha=x,y,z}A_{k,\alpha}t_{k,\alpha}^\dagger t_{k,\alpha}+\sum_{k,\alpha=x,y,z}\frac{B_{k,\alpha}}{2}(t_{k,\alpha}^\dagger t_{-k,\alpha}^\dagger+\text{H.c.}). \quad (9)$$

The coefficients in the above equation are

$$A_{k,z}=J_\perp+\delta J\xi_k, \quad A_{k,(x,y)}=\frac{J_\perp}{2}(1+\Delta)+J\xi_k,$$

$$B_{k,z}=\delta J\xi_k, \quad B_{k,(x,y)}=J\xi_k,$$

$$\xi_k=[\cos k_x+\cos k_y]/2. \quad (10)$$

Also for H_3, we obtain

$$H_3 = iJ\sum_{k_1,k_2,k_3=k_1+k_2}\xi_{k_1}(t_{x,k_1}^\dagger t_{y,k_2}^\dagger t_{z,k_3}-t_{x,k_1}^\dagger t_{z,k_2}^\dagger t_{y,k_3}+t_{y,k_1}^\dagger t_{z,k_2}^\dagger t_{x,k_3}-t_{y,k_1}^\dagger t_{x,k_2}^\dagger t_{z,k_3}+\delta t_{z,k_1}^\dagger t_{x,k_2}^\dagger t_{y,k_3}-\delta t_{z,k_1}^\dagger t_{y,k_2}^\dagger t_{x,k_3}). \quad (11)$$

Because H_3 and H_4 are of higher order in triplet operators, they will lead to only small corrections in the spectrum. Therefore, the effect of H_3 and H_4 may be taken into account on a mean field level.

The dominant contribution to the renormalization of the spectrum comes from the constraint where only one of the triplet states can be excited on every site (the hard core condition) $t_{\alpha i}^\dagger t_{\beta i}^\dagger=0$, which can be taken into account by introducing an infinite on-site repulsion between the bosons,

$$H_U = U\sum_{i,\alpha,\beta}t_{\alpha i}^\dagger t_{\beta i}^\dagger t_{\beta i}t_{\alpha i}, \quad U\to\infty. \quad (12)$$

Writing H_U in terms of Fourier transforms of boson operators, we obtain

$$H_U = U\sum_{k,k',q,\alpha,\beta}t_{\alpha k+q}^\dagger t_{\beta k'-q}^\dagger t_{\beta k'}t_{\alpha k}. \quad (13)$$

III. GREEN'S FUNCTION FORMALISM IN THE BOSONIC TRIPLET GAS

The second part of H_2 leads to the noninteracting normal Green's function and in addition to anomalous Green's function. Therefore, we introduce the single particle Green's function for the noninteracting Hamiltonian, which helps us to obtain the interacting (H_U) Green's function for the triplet operators by using Dyson's equation. Implementing the Bogoliubov transformation $t_{k,\alpha}=u_{k,\alpha}\tilde{t}_{k,\alpha}+v_{k,\alpha}\tilde{t}_{-k,\alpha}^\dagger$, we obtain $\omega_{k,\alpha}^2=A_{k,\alpha}^2-B_{k,\alpha}^2$ for the excitation spectrum at the quadratic level (H_2 only). The Bogoliubov coefficients are $u_{k,\alpha}^2(v_{k,\alpha}^2)=(-)\frac{1}{2}+\frac{A_{k,\alpha}}{2\omega_{k,\alpha}}$. The noninteracting normal triplet Green's function is $G_\alpha^n(k,t)=-i\langle T[t_{k,\alpha}(t)t_{k,\alpha}^\dagger(0)]\rangle$ and the anomalous Green's function is $G_\alpha^a(k,t)=-i\langle T[t_{k,\alpha}^\dagger(t)t_{-k,\alpha}^\dagger(0)]\rangle$. Together, we have

$$G_\alpha^n(k,\omega)=\frac{u_{k,\alpha}^2}{\omega-\omega_{k,\alpha}+i\eta}-\frac{v_{k,\alpha}^2}{\omega+\omega_{k,\alpha}-i\eta}, \quad (14)$$

$$G_\alpha^a(k,\omega)=\frac{u_{k,\alpha}v_{k,\alpha}}{\omega-\omega_{k,\alpha}+i\eta}-\frac{v_{k,\alpha}u_{k,\alpha}}{\omega+\omega_{k,\alpha}-i\eta}. \quad (15)$$

The interacting Green's functions are obtained from Dyson's equation for each Green's function (anomalous or normal). The perturbation expansion for the interacting Green's functions (for each polarization component of the triplet bosons) is written as

$$\bar{G}(k,\omega)=\overline{G^0}(k,\omega)[1-\overline{G^0}(k,\omega)\bar{\Sigma}(k,\omega)]^{-1}. \quad (16)$$

The interacting Green's function $[\bar{G}(k,\omega)]$ and the self-energy $[\bar{\Sigma}(k,\omega)]$ are 2×2 matrices

$$\bar{G}(k,\omega)=\begin{pmatrix}G_n(k,\omega) & G_a(k,\omega)\\ G_a(k,\omega) & G_n(-k,-\omega)\end{pmatrix},$$

$$\bar{\Sigma}(k,\omega)=\begin{pmatrix}\Sigma_n(k,\omega) & \Sigma_a(k,\omega)\\ \Sigma_a(k,\omega) & \Sigma_n(-k,-\omega)\end{pmatrix}. \quad (17)$$

The matrix form of Green's function can be simply expressed by $\bar{G}(k,t)=\langle T[\Phi(k,t)\Phi^\dagger(k,0)]\rangle$, where $\Phi^\dagger(k,t)=[t^\dagger(k,t)\ t(-k,t)]$ is the row vector. Inserting the elements of Eqs. (14) and (15) into Eq. (16), the normal and anomalous interacting Green's function will be obtained by

$$G_{n,\alpha}(k,\omega)=\frac{\omega+A_{k,\alpha}+\Sigma_{n,\alpha}(-k,-\omega)}{[\omega+A_{k,\alpha}+\Sigma_{n,\alpha}(k,-\omega)][\omega-A_{k,\alpha}-\Sigma_{n,\alpha}(k,\omega)]+[B_k+\Sigma_{a,\alpha}(k,\omega)]^2},$$

$$G_{a,\alpha}(k,\omega)=\frac{B_{k,\alpha}+\Sigma_{a,\alpha}(k,\omega)}{[\omega+A_{k,\alpha}+\Sigma_{n,\alpha}(k,-\omega)][\omega-A_{k,\alpha}-\Sigma_{n,\alpha}(k,\omega)]+[B_k+\Sigma_{a,\alpha}(k,\omega)]^2}. \tag{18}$$

The normal and anomalous self-energy are due to boson interactions H_3 and H_U and will be discussed in the next sections. Here, we are interested to find the one particle excitations which are the poles of the normal triplet Green's function. The Green's function should be separated into the bosonic excitation contribution and incoherent background (including collective modes). Indeed, poles of the one particle Green's function of the triplet bosons result in low energy excitations of the Hamiltonian which vanish close to the critical point. To get the single particle excitation, the self-energy is expanded for low energies leading to

$$G_{n,\alpha}(k,\omega)=\frac{\omega+A_{k,\alpha}+\Sigma_{n,\alpha}(k,0)-\omega\partial_\omega\Sigma_{n,\alpha}(k,0)}{D+[B_{k,\alpha}+\Sigma_{a,\alpha}(k,0)]^2},$$

$$D\equiv D_1\cdot D_2,$$

$$D_1\equiv[\omega+A_{k,\alpha}+\Sigma_{n,\alpha}(k,0)-\omega\partial_\omega\Sigma_{n,\alpha}(k,0)],$$

$$D_2\equiv[\omega-A_{k,\alpha}-\Sigma_{n,\alpha}(k,0)-\omega\partial_\omega\Sigma_{n,\alpha}(k,0)]. \tag{19}$$

Splitting Eq. (19) into partial fractions leads to the single particle (sp) parts

$$G^{sp}_{n,\alpha}(k,\omega)=\frac{Z_{k,\alpha}U^2_{k,\alpha}}{\omega-\Omega_{k,\alpha}+i\eta}-\frac{Z_{k,\alpha}V^2_{k,\alpha}}{\omega+\Omega_{k,\alpha}-i\eta}, \tag{20}$$

where the renormalized triplet spectrum and the renormalized single particle weight constants are given by

$$\Omega_{k,\alpha}=Z_{k,\alpha}\sqrt{[A_{k,\alpha}+\Sigma_{n,\alpha}(k,0)]^2-[B_{k,\alpha}+\Sigma_{a,\alpha}(k,0)]^2},$$

$$Z^{-1}_{k,\alpha}=1-\left(\frac{\partial\Sigma_{n,\alpha}}{\partial\omega}\right)_{\omega=0},$$

$$U^2_{k,\alpha}(V^2_{k,\alpha})=(-)\frac{1}{2}+\frac{Z_{k,\alpha}[A_{k,\alpha}+\Sigma_{n,\alpha}(k,0)]}{2\Omega_{k,\alpha}}. \tag{21}$$

The renormalized weight constant is indeed the residue of the single particle pole in the Green's function. For the noninteracting system, it is equal to 1.

IV. CALCULATION OF BOSON SELF-ENERGY DUE TO H_U AND H_3

Since the Hamiltonian H_U in Eq. (13) is short ranged and U is large, the ladder diagram approach[18] may be applied. This approach is suitable to solve Dyson's equation in order to get the boson Green's function. Formally, this is quite similar to Ref. 13, however, technically more demanding due to the effect of anisotropies (δ,Δ).

Now, we should impose the hard core repulsion due to the Hamiltonian H_U and obtain the interacting normal Green's function by Dyson's equation. First, we introduce the scattering amplitude $\Gamma_{\alpha\beta,\gamma\delta}(k_1,k_2;k_3,k_4)$ of triplet bosons, where $k_i=(\vec{k}_i,k^0_i)$. The ladder approximation satisfies a Bethe–Salpeter equation which is shown in Fig. 1 and written in Eq. (22). The scattering amplitude or self-energy for the two particle Green's function depends on the total energy and momentum of the incoming particles $\vec{K}=\vec{p}_1+\vec{p}_2$. The nonretarded and local character of U leads to $\Gamma_{\alpha\beta,\gamma\delta}=\Gamma\delta_{\alpha\gamma}\delta_{\beta\delta}$. The basic approximation made in the derivation of $\Gamma(K)$ is that we neglect all anomalous scattering vertices, which are present in the theory due to the existence of anomalous Green's functions. For the scattering amplitude shown in Fig. 1, according to the Feynman rules in momentum space, we can write [note $p\equiv(p_0,\vec{p})$]

$$\Gamma_{\alpha\beta,\alpha\beta}(p_1p_2;p_3p_4)=U(p_1-p_3)+i(2\pi)^{-4}\int[d^4QU(Q-p_2)G^0_{\alpha\alpha}(Q)\times G^0_{\beta\beta}(p_1+p_2-Q)\Gamma_{\alpha\beta,\alpha\beta}(p_1+p_2-Q,Q;p_3p_4)]. \tag{22}$$

In the above equation, U is independent of momentum and energy. Consequently, the Γ function depends only on the sum of the incoming momentum and energy and does not depend separately on the momentum and energy of the incoming particles. Therefore, $p_1+p_2=p_3+p_4\equiv K=(\vec{K},\omega)$, which simplifies Eq. (22) to

$$\Gamma_{\alpha\beta,\alpha\beta}(\vec{K},\omega)=U+i(2\pi)^{-4}\int d^4QUG^0_{\alpha\alpha}(Q)G^0_{\beta\beta}(\vec{K}-Q)\Gamma_{\alpha\beta,\alpha\beta}(\vec{K},\omega). \tag{23}$$

However, the key observation is that all anomalous contributions are suppressed by an additional small parameter present in the theory—the density of the triplet excitation $n_i=\Sigma_\alpha\langle t^\dagger_{\alpha i}t_{\alpha i}\rangle=N^{-1}\Sigma_{\vec{q},\alpha}v^2_{q,\alpha}\approx 0.1$. Indeed, both terms of the anomalous scattering matrix are proportional to $v^2_{q,\alpha}$ which are neglected. By replacing the noninteracting normal Green's function [Eq. (14)] in the Bethe–Salpeter equation [Eq. (23)] and taking the limit $U\to\infty$, we obtain the scattering matrix in the form (see Appendix A)

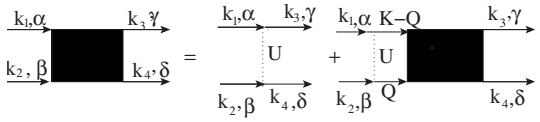

FIG. 1. Ladder diagram for the triplet boson scattering amplitude $\Gamma_{\alpha\beta,\gamma\delta}(k_1,k_2;k_3,k_4)$.

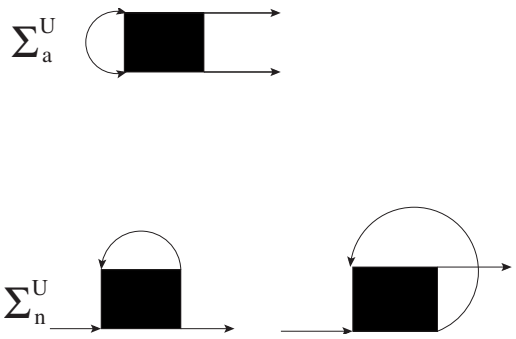

FIG. 2. Diagrams for the normal and anomalous single particle self-energies due to hard core term H_U and using the two particle scattering amplitude in Fig. 1.

$$\Gamma_{\alpha\beta,\alpha\beta}(\vec{K},\omega) = -\left(\frac{1}{N}\sum_{\vec{q}}\frac{u^2_{q,\alpha}u^2_{K-q,\beta}}{\omega-\omega_{q,\alpha}-\omega_{K-q,\beta}} - \frac{v^2_{q,\alpha}v^2_{K-q,\beta}}{\omega+\omega_{q,\alpha}+\omega_{K-q,\beta}}\right)^{-1}. \quad (24)$$

Now, we can calculate the single particle self-energy (Fig. 2) of bosons by utilizing the two particle self-energy (Γ) shown in Fig. 1 and obtained in Eq. (24).[18] Because of the strong interaction between the triplet bosons, we should carry out the expansion in Dyson's equation to infinite order. Therefore, $\Sigma^U_{\alpha\alpha}(k)$ is written as

$$\Sigma^U_{\alpha\alpha}(k) = \sum_{\gamma\beta}\int_{-\infty}^{\infty} d^4p\Gamma_{\alpha\beta,\gamma\delta}(p,k;k,p)G^0_{\gamma\beta}(p) + \sum_{\beta\delta}\int_{-\infty}^{\infty} d^4p\Gamma_{\alpha\beta,\gamma\delta}(p,k;p,k)G^0_{\delta\beta}(p). \quad (25)$$

(Note that $\Gamma_{\alpha\beta,\gamma\delta}=\Gamma_{\alpha\beta,\alpha\beta}\delta_{\alpha\gamma}\delta_{\beta\delta}$ and U is frequency and momentum independent.) For example, the x component of the self-energy is written as

$$\Sigma^U_{xx}(k) = 2\left(\frac{i}{2\pi}\right)^4\int_{-\infty}^{\infty} d^4p\Gamma_{xx,xx}(p+k)G^0_{xx}(p) + \left(\frac{i}{2\pi}\right)^4\int_{-\infty}^{\infty} d^4p\Gamma_{xz,xz}(p+k)G^0_{zz}(p) + \left(\frac{i}{2\pi}\right)^4\int_{-\infty}^{\infty} d^4p\Gamma_{xy,xy}(p+k)G^0_{yy}(p). \quad (26)$$

In the above equation, the first and third terms are similar. We integrate over the internal energy in complex plane on a contour in the upper half plane since $G^0(p)$ [Eq. (26)] is antitime ordered. Consequently, $\Sigma^U_{xx}(k,k_0\equiv\omega)$ will be written as (N is the number of cells in the lattice)

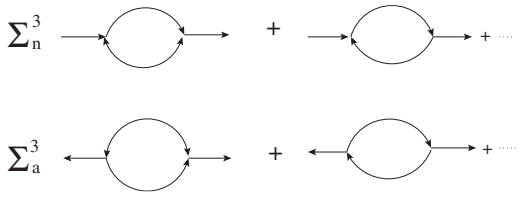

FIG. 3. One loop diagrams for normal and anomalous self-energies arising from the three point interaction H_3.

$$\Sigma^U_{xx}(k,k_0\equiv\omega) = 3\frac{i}{2\pi N}\sum_p\int_{-\infty}^{\infty} dp_0\Gamma_{xx,xx}(p+k,p_0+k_0)\frac{-v^2_{p,x}}{p_0+\omega_{p,x}-i\eta} + \frac{i}{2\pi N}\sum_p\int_{-\infty}^{\infty} dp_0\Gamma_{xz,xz}(p+k,p_0+k_0)\frac{-v^2_{p,z}}{p_0+\omega_{p,z}-i\eta} = \frac{3}{N}\sum_p v^2_{p,x}\Gamma_{xx,xx}(p+k,\omega-\omega_{p,x}) + \frac{1}{N}\sum_p v^2_{p,z}\Gamma_{xz,xz}(p+k,\omega-\omega_{p,z}). \quad (27)$$

In the dilute gas approximation, there are other diagrams which are formally at most linear in n_t (density of triplet bosons) but still numerically give contributions much smaller than Eq. (27). We should also consider the anomalous self-energy related to H_U which is obtained from the vertex function in Eq. (24). The anomalous self-energy [nondiagonal elements in the Eq. (17)] is written as (Fig. 2)

$$\Sigma^U_A = \frac{1}{N}\sum_q u_q v_q\Gamma(0,0). \quad (28)$$

The self-energy is proportional to $\Sigma_q u_q v_q$ since the vertex function is independent of k. It is then proportional to the anomalous Green's function. It is negligible as compared with the normal self-energy (diagonal parts).

We now consider the H_3 contribution in the normal and anomalous parts of the self-energy. The normal part should be added to the self-energy due to H_U. Since H_3 is much weaker than H_U, it is sufficient to obtain the second order perturbation result of Dyson's series for each component of the normal Green's function. The formula for the self-energy contribution (either anomalous or normal) is quite lengthy and has been presented in Appendix B, and the corresponding Feymann diagrams are shown in Fig. 3. The normal self-energy contribution of H_3 is proportional to u^4 which therefore dominates the anomalous one.

V. EFFECT OF H_4 ON THE RENORMALIZATION OF THE SPECTRUM

Because H_4 is composed of quartic terms in the triplet operators, its effect should be very small. It is therefore treated in mean field approximation by contracting the quartic operator products into all possible pairs. This is equivalent to take only the one loop diagrams (first order in J) into account. On the mean field level, we have $O_1O_2=\langle O_1\rangle O_2$

$+\langle O_2\rangle O_1 - \langle O_2\rangle\langle O_1\rangle$, where each O_1 and O_2 is a pair of boson triplet operator. We can write for each pair of operators

$$\langle t^\dagger_{i,\alpha} t_{j,\alpha}\rangle = \frac{i}{2\pi N}\int_{-\infty}^{\infty} d\omega \sum_k e^{ik(R_j-R_i)-i\omega 0^+} G_n^{\alpha\alpha}(k,\omega)$$

$$= \frac{1}{N}\sum_k e^{ik(R_j-R_i)} v^2_{k,\alpha},$$

$$\langle t^\dagger_{i,\alpha} t^\dagger_{j,\alpha}\rangle = \frac{1}{N}\sum_k e^{ik(R_j-R_i)} u_{k,\alpha} v_{k,\alpha}. \tag{29}$$

Thus, the effect of H_4 is to renormalize A and B coefficients defined in H_2 in the form

$$A_{k,z} \to A_{k,z} + 2J\xi_k \frac{1}{N}\sum_q (v^2_{q,x})\xi_q,$$

$$B_{k,z} \to B_{k,z} - 2J\xi_k \frac{1}{N}\sum_q (u_{q,x} v_{q,x})\xi_q,$$

$$A_{k,(x,y)} \to A_{k,(x,y)} + J\xi_k \frac{1}{N}\sum_q (\delta v^2_{q,(x,y)} + v^2_{q,z})\xi_q,$$

$$B_{k,(x,y)} \to B_{k,(x,y)} - J\xi_k \frac{1}{N}\sum_q (\delta u_{q,(x,y)} v_{q,(x,y)} + u_{q,z} v_{q,z})\xi_q. \tag{30}$$

The renormalized coefficients [Eq. (30)] will be considered to calculate the normal and anomalous self-energies which are independent of energy (nonretarded in time representation). The self-consistent solution of Eqs. (24), (27), (B1)–(B4), (30), and (21) describes the quantum critical behavior of this model which will be discussed in the following sections.

VI. QUANTUM CRITICAL POINT AND THE GAP EXPONENT

Close to the critical point, quantum fluctuations exist over all length scales which define a scaling behavior for the physical quantities. The correlation length scales like $\xi \sim |J_\perp - J_{\perp c}|^\nu$, where ν is a critical exponent. This is related to the scaling behavior of the excitation gap in the Kondo singlet phase which vanishes like

$$E_g \sim |J_\perp - J_{\perp c}|^\phi, \tag{31}$$

as $J_\perp$ approaches its critical value $J_{\perp c}$. Here, ϕ is called the gap exponent which is connected to the universality class of the quantum critical point. From general scaling arguments, one expects $\phi = \nu z$, where z is the dynamical critical exponent that determines the effective dimension D_{eff} of the model at $T=0$ according to $D_{eff}=D+z$. The spin excitation gap is defined by the energy of triplet excitations with x polarization close to the antiferromagnetic wave vector q_0. In its vicinity ($|k-q_0| \ll 1$), the triplet dispersion can be approximated by

$$\omega_{k,x} = \sqrt{E_g^2 + c_x^2 (k-q_0)^2}, \tag{32}$$

where c_x is the spin wave velocity[13,19–21] and $q_0=(\pi,\pi)$. There is no analytical expression for the spectrum of excitations; therefore, we use numerical results to get the spin wave velocity. The slope of dispersion of the x-component excitations close to q_0 is calculated numerically which is the spin wave velocity c_x. To find the energy gap, we should consider the excitation energy at the wave vector q_0,

$$E_g^2 = Z_{q_0,x}(A^2_{q_0,x} - B^2_{q_0,x}), \tag{33}$$

where the renormalized constants have been obtained in the previous section,

$$A_{k,x} = \frac{J_\perp}{2}(1+\Delta) + J\xi_k + \Sigma^U_{n,x}(k) + \Sigma^3_{n,x}(k)$$

$$+ \frac{J\delta\xi_k}{N}\sum_q (Z_{q,x} v^2_{q,x} + Z_{q,z} v^2_{q,z})\xi_q,$$

$$B_{k,x} = J\xi_k + \Sigma^U_{a,x}(k) + \Sigma^3_{a,x}(k) - \frac{J\xi_k}{N}\sum_q (\delta u_{q,x} v_{q,x} + u_{q,z} v_{q,z})\xi_q. \tag{34}$$

For the values of $A_{q_0,x}$ and $B_{q_0,x}$ at the critical point, $A^c_{q_0,x} = -B^c_{q_0,x}$ holds.

The energy gap in Eq. (33) vanishes at the quantum critical point ($J_{\perp c}$) and its behavior close to this point defines the scaling in Eq. (31). We now look for the variation of the energy gap as $J_\perp$ deviates from $J_{\perp c}$, which is given by the variation of $A_{q_0,x}$ and $B_{q_0,x}$ with respect to the $J_\perp$ deviation. The deviation of $J_\perp$ from the critical point is defined by $\delta_s J_\perp \equiv J_\perp - J_{\perp c}$. Therefore, close to critical point, $A_{q_0,x}$ and $B_{q_0,x}$ can be written as

$$A_{q_0,x} = A^c_{q_0,x} + \frac{1+E_g}{2}\delta_s J_\perp + \partial\Sigma^U_{n,x}(\pi,\pi) + \partial\Sigma^3_{n,x}(\pi,\pi)$$

$$- \frac{J\delta}{N}\sum_q (Z_{q,x}\partial v^2_{q,x})\xi_q,$$

$$B_{q_0,x} = B^c_{q_0,x} + \partial\Sigma^3_{a,x}(\pi,\pi) - \frac{J}{N}\sum_q (Z_{q,x}\partial u_{q,x} v_{q,x})\xi_q, \tag{35}$$

where ∂X means the variation of X with respect to $\delta_s J_\perp$. If we substitute Eq. (35) into Eq. (33) and neglect terms quadratic in E_g, the variation of A_{q_0} and B_{q_0} must vanish,

$$\partial A_{q_0} = \frac{1+E_g}{2}\delta_s J_\perp + \delta_s\Sigma^U_{n,x}(\pi,\pi) + \partial\Sigma^3_{n,x}(\pi,\pi)$$

$$- \frac{J\delta}{N}\sum_q (Z_{q,x}\partial v^2_{q,x})\xi_q = 0,$$

$$\partial B_{q_0} = \partial \Sigma^3_{a,x}(\pi,\pi) - \frac{J}{N}\sum_q (Z_{q,x}\partial u_{q,x} v_{q,x})\xi_q = 0. \quad (36)$$

We now have to obtain the variation of each of the terms present in Eq. (35). In the first step, we calculate the variation of the self-energy related to H_U which is written as

$$\begin{aligned}\partial \Sigma^U_x(\pi,\pi) = 3\int \frac{d^2q}{(2\pi)^2}\partial v^2_{q,x}\Gamma_{xx,xx}(q+q_0,-\omega_{q,x}) \\ + 3\int \frac{d^2q}{(2\pi)^2} v^2_{q,x}\partial\Gamma_{xx,xx}(q+q_0,-\omega_{q,x}) \\ + \int \frac{d^2q}{(2\pi)^2}\partial v^2_{q,z}\Gamma_{xz,xz}(q+q_0,-\omega_{q,z}) \\ + \int \frac{d^2q}{(2\pi)^2} v^2_{q,z}\partial\Gamma_{xz,xz}(q+q_0,-\omega_{q,z}), \quad (37)\end{aligned}$$

where $\partial v^2_{p,z}=0$. Indeed for $0 \leqslant \delta < 1$, the z component of the spectrum has a finite gap when the x component becomes gapless at the quantum critical point. The main contribution to the first integral in Eq. (37) comes from the small momenta ($q \sim E_g \ll 1$) since

$$\partial v^2_{q,x} = \frac{1}{2}\left(\frac{\partial A_{q,x}}{\omega_{q,x}} + A_{q,x}\partial\left[\frac{1}{\omega_{q,x}}\right]\right) \approx -\frac{A^c_{q_0,x}E_g^2}{2[E_g^2 + c_x^2(q-q_0)^2]^{3/2}}, \quad (38)$$

and according to Eq. (36) the variation $\partial A_{q,x}$ in this formula vanishes. We define the value of quantity X at the critical point by X^c. Taking into account the first correction to the triplet density n_b, the x component of the vertex function can be written for small q (see Ref. 22),

$$\Gamma_{xx,xx}(q,-\omega_{q,x}) \approx \Gamma^c_{xx,xx} + \frac{{\Gamma^c_{xx,xx}}^2 A^c_{0,x}}{4\pi c_x^2}\ln q, \quad (39)$$

where $\Gamma_{xx,xx}(0,0)=\Gamma^c_{xx,xx}$. The substitution of Eq. (39) into Eq. (37) and replacing $q \to E_g/J$ in the first integral of Eq. (37), leads to the following equation for the variation of H_U self-energy:

$$\begin{aligned}\partial \Sigma^U_x(\pi,\pi) = -\frac{3A^c_{q_0,x}E_g}{4\pi c_x^2}\left(\Gamma^c_{xx,xx} + \frac{{\Gamma^c_{xx,xx}}^2 A^c_{0,x}}{4\pi c_x^2}\ln\frac{E_g}{J}\right) \\ + \frac{1}{3}\Gamma'_{xz,xz} n_b \delta_s J_\perp + \Gamma'_{xx,xx} n_b \delta_s J_\perp. \quad (40)\end{aligned}$$

In the second and fourth terms of Eq. (37), we have $\Gamma'_{\alpha\beta,\alpha\beta} = \frac{\delta\Gamma_{\alpha\beta,\alpha\beta}(q,-\omega_q)}{\delta J_\perp}$ and n_b is the density of triplet excitations at the critical point. Now, we consider the effect of H_3 on the gap exponent. According to Appendix B, the variation of the self-energy contribution of H_3 is given by

$$\begin{aligned}\partial \Sigma^3_{n,x}(\pi,\pi) = \frac{J^2}{2N}[\chi u^c_{q=0,z} v^c_{q=0,z} + \varphi (v^c_{q=0,z})^2 \\ + \varphi (u^c_{q=0,z})^2]\sum_q \partial\left(\frac{1+2v^2_{q,x}}{\omega_{q,z}+\omega_{q,x}}\right), \quad (41)\end{aligned}$$

where $\chi=-(4\delta+2+2\delta^2)$, $\varphi=-(2\delta+1+\delta^2)$. Since in the vicinity of critical point $\omega_{x,q_0} \ll \omega_{z,q_0}$, the variation of Eq. (41) gives

$$\begin{aligned}\partial\left(\frac{1}{\omega_{q,x}+\omega_{q,z}}\right) \\ = -\frac{E_g^2 A^c_{q_0,x}}{4[E_g^2 + c_x^2(q-q_0)^2]^{1/2}[\omega_{q,z} + \sqrt{E_g^2 + c_x^2(q-q_0)^2}]^2}. \quad (42)\end{aligned}$$

The integral of Eq. (42) multiplied by $1+2v^2_{q,x}$ is proportional to $E_g^2 \ln E_g$, which can be neglected compared with the first term in Eq. (40). Therefore, we can restrict to the variation of $1+2v^2_{q,x}$. Then, the dominant contribution of Eq. (41) is given by

$$\partial \Sigma^3_{n,x}(\pi,\pi) = -\frac{A^c_{q_0,x} J^2\{(u^c_{0,z}v^c_{0,z})\chi + [(u^c_{0,z})^2 + (v^c_{0,z})^2]\varphi\}}{4\pi c_x^2 \omega^c_{0,z}} E_g. \quad (43)$$

We then calculate the last variation of the first expression in Eq. (35),

$$J\frac{1}{N}\sum_q (\delta Z_{q,x}\partial v^2_{q,x})\xi_q = -\frac{\delta Z_0 J A^c_{q_0,x}}{\pi c_x^2} E_g. \quad (44)$$

Let us define the following expressions:

$$\lambda \equiv \frac{3A^c_{q_0,x}\Gamma^c_{xx,xx}}{4\pi c_x^2},$$

$$\theta \equiv \frac{A^c_{q_0,x} J^2\{(u^c_{0,z}v^c_{0,z})\chi + [(u^c_{0,z})^2 + (v^c_{0,z})^2]\varphi\}}{4\pi c_x^2 \omega^c_{0,z}},$$

$$\mu \equiv \frac{\delta J A^c_{q_0,x}}{\pi c_x^2},$$

$$\sigma \equiv \frac{1}{3}\Gamma'_{xz,xz} n_b \delta J_\perp + \Gamma'_{xx,xx} n_b \delta J_\perp. \quad (45)$$

From the substitution of Eqs. (44), (43), and (40) into the first expression of Eq. (36), we get the following equation:

$$E_g = \frac{\left(\frac{1+E_g}{2} + \sigma\right)\delta_s J_\perp}{\lambda + \theta + \mu}\left[1 - \frac{\lambda A^c_{q_0,x}\Gamma^c_{xx,xx}}{4\pi c_x^2(\lambda+\theta+\mu)}\ln\frac{\delta_s J_\perp}{J}\right]. \quad (46)$$

To find the gap exponent ϕ, we should consider $E_g = (\delta_s J_\perp)^\phi$. Indeed, ϕ is the smallest exponent that can be considered for E_g. Finally, we obtain

TABLE I. The critical point $[(\frac{J_\perp}{J})_c]$ at which the singlet gap vanishes for different values of intersite anisotropy (Δ) and $\delta=0$. The second row shows the result from Green's function approach and the third row gives the mean field values for the critical point (Ref. 14). The gap exponent in the fourth row is obtained from the numerical evaluation of Eq. (47). The accuracy of data is ± 0.005.

Δ	0.0	0.2	0.4	0.6	0.8	0.9	1.0
$(\frac{J_\perp}{J})_c$ (Green's function)	3.01	2.55	2.17	1.90	1.72	1.64	1.55
$(\frac{J_\perp}{J})_c$ (mean field)	2.86	2.38	2.04	1.78	1.59	1.51	1.43
ϕ (gap exponent)	0.83	0.83	0.83	0.82	0.82	0.82	0.82

$$\phi = 1 - \frac{\lambda A^c_{q_0,x}\Gamma^c_{xx,xx}}{4\pi c_x^2(\lambda+\theta+\mu)}. \tag{47}$$

The last equation is obtained using $\omega_{x,q_0} \ll \omega_{z,q_0}$. For the isotropic case, $\omega_{x,q_0}=\omega_{z,q_0}\equiv\omega_{q_0}$, where the expression for $\Sigma^U_x(\pi,\pi)$ should be changed. The final result for the gap exponent of the isotropic case ($\delta=\Delta=1$) is given by

$$\phi = 1 - \frac{\lambda A^c_{q_0}\Gamma^c}{4\pi c^2(\lambda+\mu+\theta)}. \tag{48}$$

In the above equation, we have

$$A^c_{q_0,x} = A^c_{q_0,z} \equiv A^c_{q_0},$$

$$\lambda \equiv \frac{A^c_{q_0}\Gamma^c}{\pi c^2},$$

$$\mu \equiv 2\frac{JA^c_{q_0}}{\pi c^2},$$

$$\theta \equiv \frac{A^c_{q_0}J^2\{16(u^c_0v^c_0)+8[(u^c_0)^2+(v^c_0)^2]\}}{4\pi c^2\omega^c_0}. \tag{49}$$

We have summarized the numerical values of the gap exponent for different anisotropies (δ,Δ) in Tables I and II.

VII. QUANTUM CRITICAL PHASE DIAGRAMS: NUMERICAL RESULTS

Our approach is based on the strong coupling limit, $J_\perp/J\to\infty$. In this limit, the ground state has singlet character and a finite energy gap exists to the lowest excited triplet state. The increase of intersite exchange coupling (J) or the decrease of on-site exchange ($J_\perp$) lowers the excitation gap which eventually vanishes. The position where the bosonic excitation gap vanishes defines the quantum critical point. At this point, the condensation of a triplet takes place which induces the antiferromagnetic order. The single particle excitation energy should be obtained in a self-consistent solution of Eqs. (24), (27), (B1)–(B4), (30), and (21). We should first replace

$$u_{k,\alpha}\to\sqrt{Z_{k,\alpha}}U_{k,\alpha}, v_{k,\alpha}\to\sqrt{Z_{k,\alpha}}V_{k,\alpha}$$

in the self-energies of H_U, H_3 and the renormalization expressions in Eq. (30). From an initial guess for $Z_{k,\alpha}, \Sigma_{n,\alpha}(k,0), \Sigma_{a,\alpha}(k,0)$ by using Eq. (21), we obtain corrected excitation energy and the renormalized Bogoliubov coefficients (u,v). We repeat the procedure until the difference between the excitation energies in two consecutive steps is smaller than an acceptable error. The exponent of the gap is given by Eq. (47), which is calculated from the vertex function and spin wave velocity at the critical point and at the antiferromagnetic wave vector $Q=(\pi,\pi)$. We will discuss the numerical results of our calculations in the next subsections for the XY case, i.e., $\delta=0$ and various sizes of on-site exchange anisotropy $0\leqslant\Delta\leqslant 1$ and likewise for $\Delta=1$ with various values of the intersite exchange anisotropy $0\leqslant\delta\leqslant 1$.

A. *XY* case: $\delta=0$

In the XY case, the z component of single particle excitation has approximately a dispersionless value $\omega_z(k)=\omega_0$. For the other components of excitations $(\omega_x=\omega_y)$, the dispersion relation shows a minimum at the reciprocal vector at the corner of the Brillouin zone (BZ), e.g., $Q=(\pi,\pi)$. In Fig. 4, we have plotted the energy gap $(E_g/J_\perp)$ versus control

TABLE II. The critical point $[(\frac{J_\perp}{J})_c]$ at which the singlet gap vanishes for different values of intersite anisotropy (δ) and $\Delta=1$. The second row shows the result from Green's function approach and the third row is the mean field values for the critical point. The gap exponent in the fourth row comes from the numerical evaluation of Eqs. (47) and (48). The accuracy of data is ± 0.005.

δ	0.0	0.2	0.4	0.6	0.8	0.9	1.0
$(\frac{J_\perp}{J})_c$ (Green's function)	1.55	1.54	1.54	1.52	1.49	1.47	1.41
$(\frac{J_\perp}{J})_c$ (mean field)	1.43	1.43	1.41	1.39	1.32	1.30	1.16
ϕ (gap exponent)	0.82	0.82	0.81	0.81	0.80	0.78	0.73

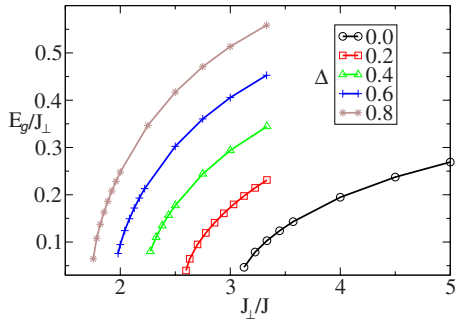

FIG. 4. (Color online) The energy gap $(E_g/J_\perp)$ versus control parameter $(J_\perp/J)$ in the two-dimensional lattice for $\delta=0$ and different values Δ.

parameter $J_\perp/J$. For all values of Δ, the gap vanishes at the critical point $(\frac{J_\perp}{J})_c$, where the transition from Kondo singlet to the antiferromagnetic phase occurs. We have presented the numerical values of the critical point in Table I for $\delta=0$ and different values of intersite anisotropy, $\Delta=0.0,0.2,0.4,0.6,0.8,0.9,1.0$. In this case, the critical points $(J_\perp/J)_c$ have also been plotted in Fig. 6 versus Δ (solid line). In Table I, we have also compared the critical point with the mean field results.[14] The gap exponent for different anisotropies have also been presented in Table I and Fig. 7. Our results in this case show that the anisotropy in the local interaction (Δ) does not change the qualitative behavior of the Kondo necklace model on the two-dimensional (2D) lattice. This is concluded from numerical values for the gap exponent ϕ which are independent of Δ.

B. General anisotropic case $\delta\neq 0$

To study the effect of a nonzero anisotropy $\delta\neq 0$ in the itinerant part, we consider only the isotropic case of the local Kondo interactions, i.e., $J_{\perp x}=J_{\perp z}=J_\perp$ $(\Delta=1)$. All of the three excitations show k dependence in this case. The minimum excitation energy at Q wave vector defines the energy gap. For $0\leqslant\delta\leqslant 1$, we have $E_g^x<E_g^z$; therefore, we have plotted $E_g^x/J_\perp$ versus $J_\perp/J$ in Fig. 5. In contrast to the case of local anisotropy, the effect of intersite anisotropy on the critical point is weak and $(J_\perp/J)_c$ changes only slightly. In Table II and Fig. 6, we have shown the calculated values of the critical point for different δ. We have also presented the gap

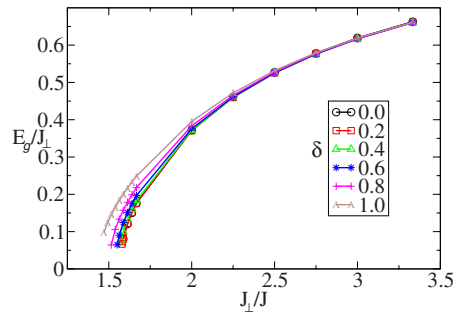

FIG. 5. (Color online) The energy gap $(E_g/J_\perp)$ versus control parameter $(J_\perp/J)$ in the two-dimensional lattice for $\Delta=1$ and different values δ.

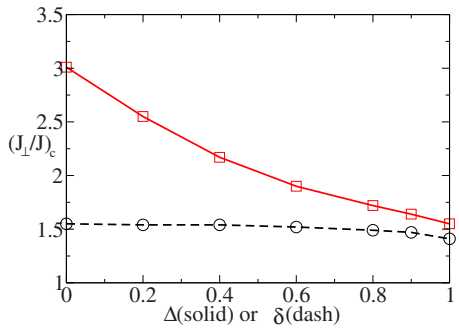

FIG. 6. (Color online) Dependence of the critical point $(J_\perp/J)_c$ on the local (Δ, solid line) and itinerant (δ, dashed line) anisotropies. For the solid line, $\delta=0$, and for the dashed line, $\Delta=1$. The numerical values are given in Tables I and II.

exponent for each anisotropy in Table II and as a plot in Fig. 7. We observe a rapid decrease of ϕ on approaching the isotropic case $(\delta=1)$. In this case, another soft mode (ω_z) is added to the excitations at the critical point and one needs a larger hopping strength (J) to reach the quantum critical point. Moreover, the symmetry changes from $U(1)$ for $0\leqslant\delta<1$ to SU(2) at $\delta=1$. Despite the weak dependence of the critical point on the anisotropy (δ), the critical exponent of the gap changes with δ, which is more pronounced at $\delta=1$. However, the whole region of $0\leqslant\delta<1$ can be considered in a single universality class where the gap exponent changes slightly, while the change of exponent at $\delta=1$ signifies a different universality class by restoring the full spin rotational symmetry.

VIII. DISCUSSION AND CONCLUSION

In this work, we have carried the analysis of quantum critical behavior of the 2D anisotropic Kondo necklace model beyond the previous mean field treatment. The constraint on the bosonic excitations has been implemented with the help of a hard core boson term at every site instead of applying a global constraint by introducing a chemical potential in the mean field approach.[14,15]

The comparison of quantum critical points $(J_\perp/J)_c$ $(\delta=1)$ as a function of Δ in Table I shows that deviations of the

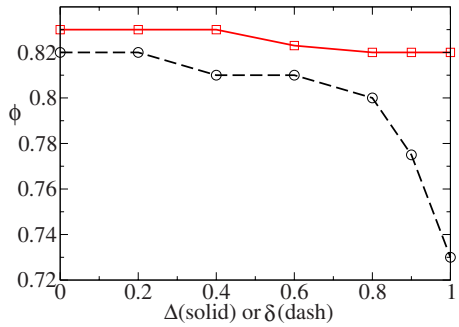

FIG. 7. (Color online) Dependence of the critical exponent (ϕ) on the local (Δ, solid line) and itinerant (δ, dashed line) anisotropies. For the solid line, $\delta=0$, and for the dashed line, $\Delta=1$. The numerical values are given in Tables I and II.

two methods are quite small, up to 10% at the most. They are somewhat larger for the complementary case ($\Delta=1$) as a function of δ (up to $\sim 17\%$), especially when the isotropic case $\delta=1$ is approached. The real difference and the advantage of the Green's function method appear when considering the critical exponent ϕ of the excitation gap E_g. In the mean field treatment, the exponent is always $\phi=1$ independent of the anisotropies (Figs. 2 and 6 in Ref. 14). On the other hand, the present Green's function approach clearly leads to nontrivial exponents $\phi<1$, as may already be seen by the direct comparison of Figs. 4 and 5 with those of Ref. 14 mentioned above. The calculated critical exponents ϕ are listed in Tables I and II and shown in Fig. 7. Generally, they lie around $\phi \simeq 0.80-0.83$. The most remarkable feature is the rapid reduction of ϕ when δ approaches the isotropic point $\delta=1$ where the universality class of the model changes from $U(1)$-xy to SU(2)-Heisenberg type. At this isotropic point, we have $\phi \simeq 0.73$. Technically, this means that three instead of two soft modes at the AF wave vector q_0 appear which causes a rapid change in the gap exponent, as described by Eqs. (47) and (48).

The critical value $(J_\perp/J)_c$ and exponent ϕ for the special isotropic case $(\delta,\Delta)=(1,1)$ have already been given in Ref. 13. From a numerical fit to the gap E_g [Eq. (31)], $(J_\perp/J)_c=1.39$ and $\phi=0.71$ were obtained, which agrees reasonably well with our values $(J_\perp/J)_c=1.41$ and $\phi=0.73$. In Ref. 13, the isotropic case was also investigated for the true bilayer Hamiltonian. If we denote the intersite coupling in the layer of localized spins $(\mathbf{S}_i)$ by λ_S, then $\lambda_S=0$ corresponds to the present KNM and $\lambda_S=J$ to the bilayer Hamiltonian. It was shown that the critical exponent ϕ for the isotropic case does not depend on λ_S. Applied to our anisotropic case, we may conjecture that the critical exponents ϕ given in Tables I and II will also be valid for the anisotropic bilayer model $\lambda_S=J$, although we have not done this calculation.

The quantum Monte Carlo results[23] give $\nu=0.71$, where ν is the critical exponent of the correlation length close to the quantum critical point of the 2D incomplete bilayer-Heisenberg model (which is exactly the isotropic Kondo necklace model). The dynamical exponent (z) relates the correlation length exponent (ν) to the gap exponent (ϕ) by $\phi=z\nu$. According to our results $\phi=0.73$, which is very close to the result for ν obtained in Ref. 23, we conclude that the dynamical exponent of the 2D isotropic Kondo necklace model is $z=1$. As a consequence, the effective dimension of the model at the QCP is $D_{eff}=D+z=3$. This means that at the QCP, the isotropic 2D KN model corresponds to the universality class of the three-dimensional classical Heisenberg model. This was also suggested in Ref. 23.

It is also worthwhile to discuss the different treatment of the bosonic constraint $s_i^\dagger s_i+\Sigma_\alpha t_{i\alpha}^\dagger t_{i\alpha}=1$ (at every site i) in the two methods in more detail since it is the source of the difference in the position of the quantum critical point $(J_\perp/J)_c$ mentioned above. Their essential difference has already been explained in Sec. II. In the mean field approach, a Lagrange term with a chemical potential μ incorporating the constraint is added to the quadratic Hamiltonian H_2. Then, the singlet and triplet boson operators in the constraint are replaced by average amplitudes $\bar{s}$ and $\bar{t}_\alpha$, where the latter is identical to zero in the nonmagnetic phase. After diagonalization of H_2, the singlet amplitude $\bar{s}$ and the chemical potential μ are determined self-consistently as a function of $J_\perp/J$ by minimizing the total energy.[14,15] This means that μ and $\bar{s}$ will be slowly varying functions of the control parameter $J_\perp/J$. On the other hand, the present Green's function approach corresponds to fixing these two parameters to $(J_\perp/J)$—independent constants given by $\bar{s}=1$ and $\mu=(J_\perp/4)(2+\Delta)$ which correspond to the mean field values for $J_\perp/J=0$. Therefore, on the level of H_2, there is no constraint implemented in the present approach. It rather appears through adding the H_U term and computing its effect on the bosonic Green's functions in the limit $U\to\infty$. One might speculate whether it would be an improvement to start from the self-consistent mean field solution for $\bar{s}$ and only then impose the further constraint with the H_U term. However, this cannot be justified easily. Once the constraints has been used in mean field level, the fluctuations of the mean field singlet and triplet amplitudes should rather be unconstrained.

However, the hard core repulsion on bosonic excitations which is imposed by H_U ensures that only one triplet can be excited on each bond. It justifies the dominant contribution to the excitation spectrum of the model. In the mean field approach, there is no restriction to have more than one triplet excitation on each bond and the constraints $s_i^\dagger s_i+\Sigma_\alpha t_{i\alpha}^\dagger t_{i\alpha}=1$ should be satisfied only when averaged over all bonds. In other words, the Green's function approach may be expected to give an improved excitation spectrum. This is the reason why the critical exponent of the excitation gap obtained by Green's function approach is more accurate.

The calculation of critical gap exponents presented here presents a contribution to understanding the quantum critical behavior of the anisotropic Kondo necklace model. An extension to the antiferromagnetic side of the quantum critical point would be desirable to allow for a full comparison with the mean field results in Ref. 14. However, this will demand an even larger technical effort than in the present work.

APPENDIX A

The triplet scattering vertex in Eq. (23) is determined by the following equation:

$$\Gamma_{\alpha\beta,\alpha\beta}(\vec{K},\omega)=\frac{U}{1-iU(2\pi)^{-4}\int d^3\vec{Q}dQ_0 G^0_{\alpha\alpha}(Q)G^0_{\beta\beta}(K-Q)\Gamma_{\alpha\beta,\alpha\beta}(\vec{K},\omega)}. \tag{A1}$$

By substituting the normal noninteracting Green function Eq. (14) in the integral in Eq. (A1) we have

$$\int dQ_0 G^0_{\alpha\alpha}(Q) G^0_{\beta\beta}(K-Q) = \int dQ_0 \left(\frac{u^2_{\vec{Q},\alpha}}{Q_0 - \omega_{\vec{Q},\alpha} + i\delta} - \frac{v^2_{\vec{Q},\alpha}}{Q_0 + \omega_{\vec{Q},\alpha} - i\delta} \right) \left(\frac{u^2_{\vec{K}-\vec{Q},\beta}}{K_0 - Q_0 - \omega_{\vec{K}-\vec{Q},\beta} + i\delta} - \frac{v^2_{\vec{K}-\vec{Q},\beta}}{K_0 - Q_0 + \omega_{\vec{K}-\vec{Q},\beta} - i\delta} \right). \tag{A2}$$

By using Cauchy's formula and extending the above integration over the complex plane Q_0, we compute the residues of the simple poles of the integrand. We found that the terms proportional to $u^2_{\vec{K}-\vec{Q},\beta} v^2_{\vec{Q},\alpha}$ and $v^2_{\vec{K}-\vec{Q},\beta} u^2_{\vec{Q},\alpha}$ give zero contribution because one pole is above the upper half plane and the other pole is below the lower half plane. After taking the limit $U \to \infty$, then we obtain Eq. (24) for the scattering matrix.

APPENDIX B

We have the following equations for the x, z component of the normal and anomalous self-energies:

$$\begin{aligned}
\Sigma^3_{n,x}(k,0) = \frac{J^2}{2N} \sum_q \Bigg\{ & \frac{1}{\omega_{q,x} + \omega_{k+q,z}} [u_{q,x} v_{q,x} (u^2_{k+q,z} + v^2_{k+q,z})(\xi_k \xi_q - 2\delta\xi_k \xi_{k+q} - \xi^2_q + 2\delta\xi_q \xi_{k+q}) + (u^2_{q,x} u^2_{k+q,z} + v^2_{q,x} v^2_{k+q,z}) \\
& \times (-\delta^2 \xi^2_{k+q} + \delta\xi_q \xi_{k+q}) + (v^2_{k+q,z} u^2_{q,x} + u^2_{k+q,z} v^2_{q,x})(-\xi^2_k + 2\xi_k \xi_q - \xi^2_q) + u_{k+q,z} v_{k+q,z} (u^2_{q,x} + v^2_{q,x})(\delta\xi_k \xi_{k+q} - \delta^2 \xi^2_{k+q}) \\
& + 2u_{k+q,z} v_{k+q,z} u_{q,x} v_{q,x} (\xi^2_k - \delta\xi_k \xi_{k+q} - \xi_k \xi_q + \delta\xi_q \xi_{k+q})] + \frac{1}{\omega_{q,z} + \omega_{k+q,x}} [u^z_q v^z_q (u^2_{k+q,x} + v^2_{k+q,x})(\delta\xi_k \xi_q - 2\xi_k \xi_{k+q} - \delta^2 \xi^2_q \\
& + 2\delta\xi^q \xi^{k+q}) + (u^2_{q,z} u^2_{k+q,z} + v^2_{q,z} v^2_{k+q,z})(-\xi^2_{k+q} + \delta\xi_q \xi_{k+q}) + u_{k+q,x} v_{k+q,x} (u^2_{q,z} + v^2_{q,z})(\xi_k \xi_{k+q} - \xi^2_{k+q}) \\
& + 2u_{k+q,x} v_{k+q,x} u_{q,z} v_{q,z} (\xi^2_k - \delta\xi_k \xi_{k+q} - \xi_k \xi_q + \delta\xi_q \xi_{k+q}) + (v^2_{k+q,x} u^2_{q,z} + u^2_{k+q,x} v^2_{q,z})(-\xi^2_k + 2\xi_k \xi_q - \xi^2_q)] \Bigg\}.
\end{aligned} \tag{B1}$$

For the anomalous x-component self-energy, we obtain

$$\begin{aligned}
\Sigma^3_{a,x}(k,0) = \frac{J^2}{2N} \sum_q \Bigg\{ & \frac{1}{\omega_{q,x} + \omega_{k+q,z}} [u_{q,x} v_{q,x} (u^2_{k+q,z} + v^2_{k+q,z})(-\delta\xi_k \xi_{k+q} + \delta^2 \xi^2_{k+q}) + u_{k+q,z} v_{k+q,z} (u^2_{q,x} + v^2_{q,x}) \\
& \times (2\delta\xi_k \xi_{k+q} + \xi^2_q - \xi_k \xi_q - 2\delta\xi_q \xi_{k+q}) + (v^2_{k+q,z} u^2_{q,x} + u^2_{k+q,z} v^2_{q,x})(-\xi^2_k + \delta\xi_k \xi_{k+q} - \delta\xi_q \xi_{k+q} + \xi_k \xi_q) \\
& + 2u_{k+q,z} v_{k+q,z} u_{q,x} v_{q,x} (\delta^2 \xi^2_{k+q} - \delta\xi_q \xi_{k+q} + \xi^2_k + \xi^2_q - 2\xi_q \xi_k)] + \frac{1}{\omega_{q,z} + \omega_{k+q,x}} [u_{q,z} v_{q,z} (u^2_{k+q,x} + v^2_{k+q,x})(-\xi_k \xi_{k+q} + \xi^2_{k+q}) \\
& + u_{k+q,x} v_{k+q,x} (u^2_{q,z} + v^2_{q,z})(2\xi_k \xi_{k+q} + \delta^2 \xi^2_q - \delta\xi_k \xi_q - 2\delta\xi_q \xi_{k+q}) + 2u_{k+q,x} v_{k+q,x} u_{q,z} v_{q,z} (\xi^2_{k+q} - \delta\xi_q \xi_{k+q} + \xi^2_k + \delta^2 \xi^2_q - 2\delta\xi_q \xi_k) \\
& + (v^2_{k+q,x} u^2_{q,z} + u^2_{k+q,x} v^2_{q,z})(-\xi^2_k + \xi_k \xi_{k+q} - \delta\xi_q \xi_{k+q} + \delta\xi_k \xi_q)] \Bigg\}.
\end{aligned} \tag{B2}$$

Similarly, we can write the following expression for the z component of the normal self-energy:

$$\begin{aligned}
\Sigma^3_{n,z}(k,0) = \frac{J^2}{N} \sum_q & \frac{1}{\omega_{q,x} + \omega_{k+q,x}} [u_{q,x} v_{q,x} (u^2_{k+q,x} + v^2_{k+q,x})(\delta\xi_k \xi_q - 2\delta\xi_k \xi_{k+q} - \xi^2_q + 2\xi_q \xi_{k+q}) + (u^2_{q,x} u^2_{k+q,x} + v^2_{q,x} v^2_{k+q,x})(-\xi^2_{k+q} + \xi_q \xi_{k+q}) \\
& + (v^2_{k+q,x} u^2_{q,x} + u^2_{k+q,x} v^2_{q,x})(-\delta^2 \xi^2_k + 2\delta\xi_k \xi_q - \xi^2_q) + u_{k+q,x} v_{k+q,x} (u^2_{q,x} + v^2_{q,x})(\delta\xi_k \xi_{k+q} - \delta^2 \xi^2_{k+q}) \\
& + 2u_{k+q,x} v_{k+q,x} u_{q,x} v_{q,x} (\delta^2 \xi^2_k - \delta\xi_k \xi_{k+q} - \delta\xi_k \xi_q + \xi_q \xi_{k+q})].
\end{aligned} \tag{B3}$$

For the corresponding anomalous self-energy, we have

$$\begin{aligned}
\Sigma^3_{a,z}(k,0) = \frac{J^2}{N} \sum_q & \frac{1}{\omega_{q,x} + \omega_{k+q,x}} [u_{q,x} v_{q,x} (u^2_{k+q,x} + v^2_{k+q,x})(-\delta\xi_k \xi_{k+q} + \xi^2_{k+q}) + u_{k+q,x} v_{k+q,x} (u^2_{q,x} + v^2_{q,x})(2\delta\xi_k \xi_{k+q} + \xi^2_q - \delta\xi_k \xi_q - 2\xi_q \xi_{k+q}) \\
& + (v^2_{k+q,x} u^2_{q,x} + u^2_{k+q,x} v^2_{q,x})(-\delta^2 \xi^2_k + \delta\xi_k \xi_{k+q} - \xi_q \xi_{k+q} + \delta\xi_k \xi_q) + 2u_{k+q,x} v_{k+q,x} u_{q,x} v_{q,x} (\xi^2_{k+q} - \xi_q \xi_{k+q} + \delta^2 \xi^2_k + \xi^2_q - 2\delta\xi_q \xi_k)].
\end{aligned} \tag{B4}$$

*langari@sharif.edu; http://spin.cscm.ir

[1] S. Sachdev, *Quantum Phase Transitions* (Cambridge University Press, Cambridge, 1999).
[2] M. Vojta, Rep. Prog. Phys. **66**, 2069 (2003).
[3] A. C. Hewson, *The Kondo Problem to Heavy Fermions* (Cambridge University Press, New York, 1993).
[4] G. R. Stewart, Rev. Mod. Phys. **73**, 797 (2001).
[5] H. Tsunetsugu, M. Sigrist, and K. Ueda, Rev. Mod. Phys. **69**, 809 (1997).
[6] S. Doniach, Physica B & C **91**, 231 (1977).
[7] P. Sun and G. Kotliar, Phys. Rev. Lett. **95**, 016402 (2005).
[8] I. Zerec, B. Schmidt, and P. Thalmeier, Phys. Rev. B **73**, 245108 (2006).
[9] A. Schröder, G. Aeppli, R. Coldea, M. Adams, O. Stockert, H. v. Loehneysen, E. Bucher, R. Ramazashvili, and P. Coleman, Nature (London) **407**, 351 (2000).
[10] J. A. Hertz, Phys. Rev. B **14**, 1165 (1976).
[11] A. J. Millis, Phys. Rev. B **48**, 7183 (1993).
[12] Ch. Brünger and F. F. Assaad, Phys. Rev. B **74**, 205107 (2006).
[13] V. N. Kotov, O. Sushkov, Zheng Weihong, and J. Oitmaa, Phys. Rev. Lett. **80**, 5790 (1998).
[14] A. Langari and P. Thalmeier, Phys. Rev. B **74**, 024431 (2006).
[15] P. Thalmeier and A. Langari, Phys. Rev. B **75**, 174426 (2007).
[16] A. V. Chubukov, JETP Lett. **49**, 129 (1989).
[17] S. Sachdev and R. N. Bhatt, Phys. Rev. B **41**, 9323 (1990).
[18] A. L. Fetter and J. D. Walecka, *Quantum Theory of Many-Particle Systems* (McGraw-Hill, New York, 1971).
[19] Zheng Weihong, Phys. Rev. B **55**, 12267 (1997).
[20] K. Hida, J. Phys. Soc. Jpn. **61**, 1013 (1992).
[21] M. P. Gelfand, Phys. Rev. B **53**, 11309 (1996).
[22] P. V. Shevchenko and O. P. Sushkov, Phys. Rev. B **59**, 8383 (1999).
[23] Ling Wang, K. S. D. Beach, and Anders W. Sandvik, Phys. Rev. B **73**, 014431 (2006).